Supplemental Figure 1

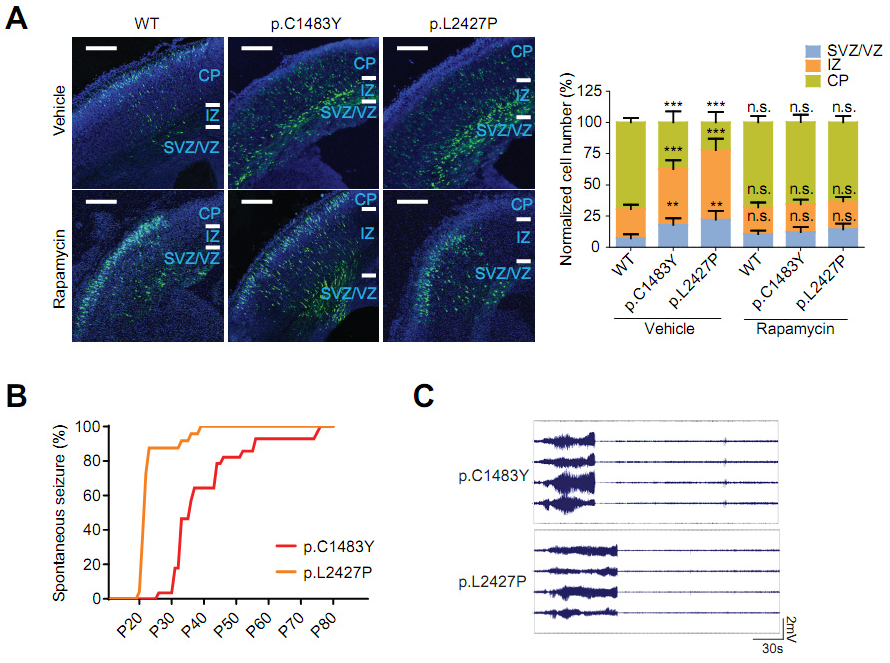

Supplemental Figure 1. Major phenotypes of FMCD reversed by mTOR inhibitor rapamycin in FMCD mice.

(**A**) Representative immunofluorescence images of migration of *in utero* electroporated neurons. GFP-positive cells represent mTOR WT (WT), mTOR p.C1483Y (p.C1483Y), and mTOR p.L2427P (p.L2427P) carrying cortical neurons from vehicle-treated (top) and rapamycin-treated (bottom) FMCD mice at E18. ** $P < 0.01$ and *** $P < 0.001$ (WT-vehicle: n = 9, p.C1483Y-vehicle: n = 9, p.L2427P-vehicle: n = 11, WT-rapamycin: n = 8, p.C1483Y-rapamycin: n = 9, p.L2427P-rapamycin: n = 5, one-way analysis of variance [ANOVA] with Bonferroni post-hoc test). Scale bars, 200 um. Mean ± SEM. CP: cortical plate, IZ: intermediate zone, SVZ/VZ: subventricular/ventricular zone.

(**B**) Cumulative graph of the percentages of spontaneous seizures elicited in the mTOR-p.C1483Y (p.C1483Y) and p.L2427P (p.L2427P) FMCD mice (left) (mTOR-p.C1483Y: n = 24, mTOR-p.L2427P: n = 29).

(**C**) Representative neocortical electroencephalographic activity of epileptic seizures in FMCD adult mice (P56-P140).

Supplemental Figure 2

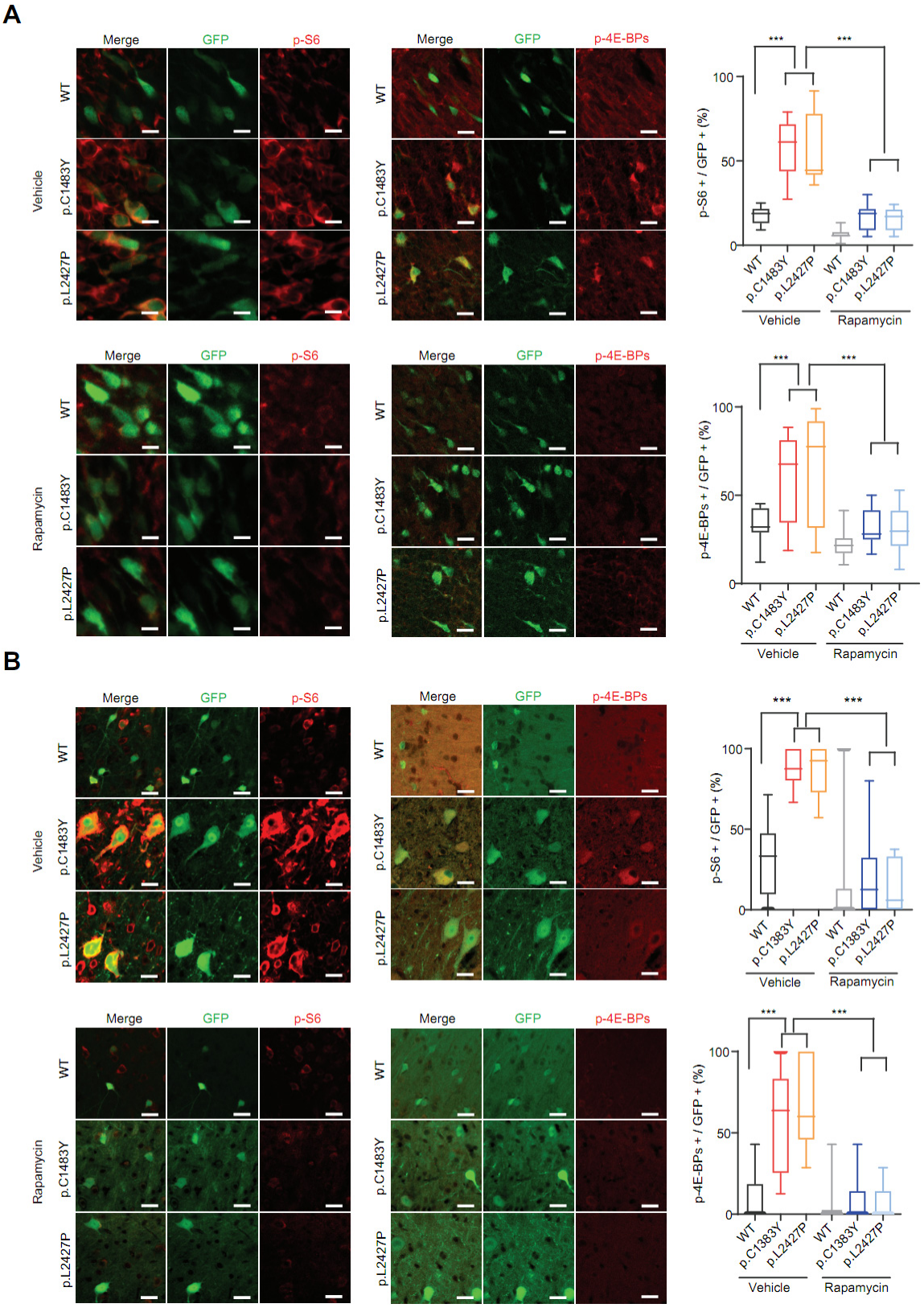

Supplemental Figure 2. Aberrant activation of mTOR kinase reversed by mTOR inhibitor rapamycin in FMCD mice.

(**A**) Representative immunofluorescence staining of p-S6 (Ser240/244) and p-4E-BPs (Thr37/46) in GFP-positive cells from vehicle-treated (top) and rapamycin-treated (bottom) FMCD mice at E18. GFP expressing cells positive for each marker were quantified in the average of two to five representative cortical regions. *** $P < 0.001$ (WT-vehicle: n = 9, p.C1483Y-vehicle: n = 9, p.L2427P-vehicle: n = 11, WT-rapamycin: n = 8, p.C1483Y-rapamycin: n = 9, p.L2427P-rapamycin: n =5, one-way ANOVA with Bonferroni post-hoc test). For p-S6, scale bars = 10 um and for p-4E-BPs, scale bars = 25 um.

(**B**) Representative immunofluorescence staining of p-S6 (Ser240/244) and p-4E-BPs (Thr37/46) in GFP-positive cells from vehicle-treated (top) and rapamycin-treated (bottom) adult FMCD mice (P56-P140). GFP expressing cells positive for each marker were quantified in the average of two to five representative cortical regions. *** $P < 0.001$ (n = 5 in each group, one-way ANOVA with Bonferroni post-hoc test). Scale bars, 25 um.

Supplemental Figure 3

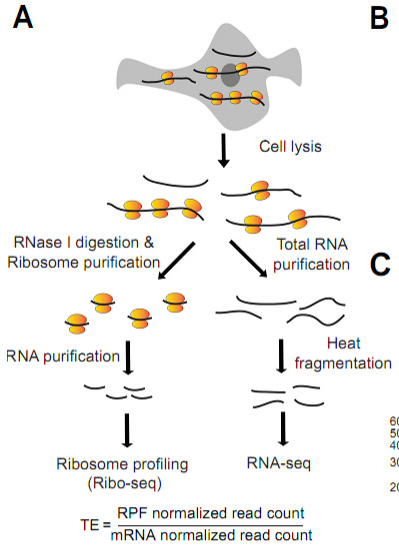

B

Total	WT (n=3)	mTOR p.C1483Y (n=3)	mTOR p.L2427P (n=3)
Cell number	6,499,030 ± 79,575	6,364,521 ± 92,811	6,711,441 ± 165,447
Embryo number	100 ± 18	84 ± 9	119 ± 14
RPF quantity (ug)	1.68 ± 0.15	1.81 ± 0.40	1.81 ± 0.16
mRNA quantity (ug)	1.48 ± 0.22	1.49 ± 0.09	1.66 ± 0.15

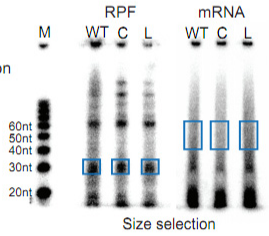

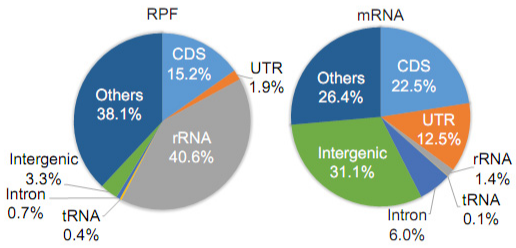

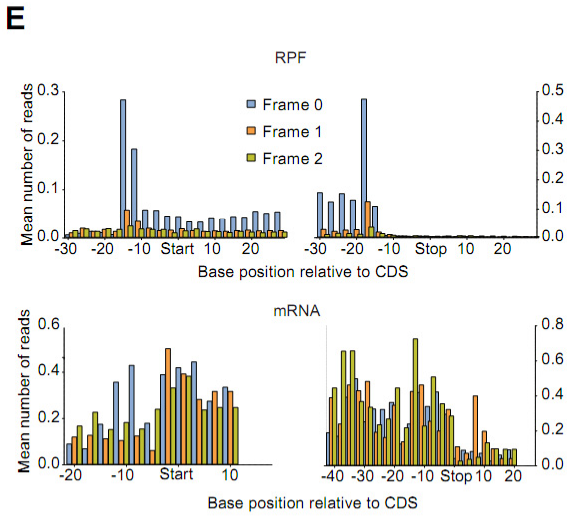

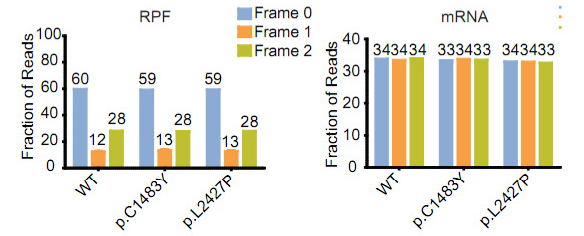

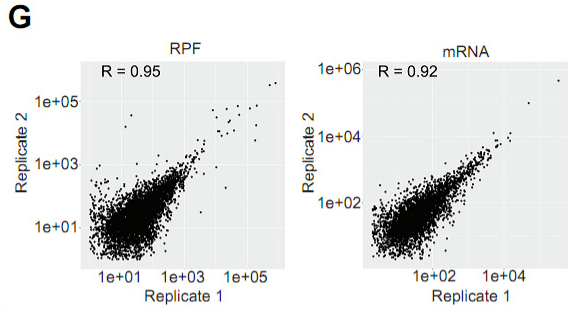

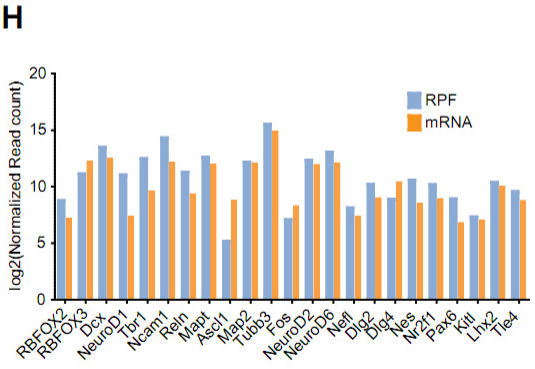

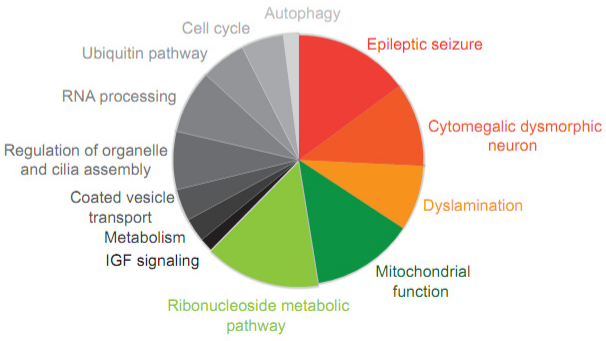

Supplemental Figure 3. Validation of the quality of Ribo-seq and RNA-seq library preparation in WT, p.C1483Y, and p.L2427P mice.

(**A)** Schematic diagram depicts the Ribo-seq and RNA-seq. TE was calculated by read count of RPF normalized by read count of mRNA of each mRNA.

(**B**) Cell number, embryo number, and amount of RPF and mRNA used for Ribo-seq and RNA-seq library preparation in FMCD mice.

(**C**) Representative images of library preparation of RPF and mRNA upon gel excision during the process of size selection. M: marker, WT: WT mice, C: p.C1483Y mice, L: p.L2427P mice.

(**D**) Mapping distributions of read counts for the assigned classes in the RPF (left) and mRNA (right) libraries.

(**E**) Density of RPF (top) and mRNA (bottom) reads near the translation start and stop codons.

(**F**) Fractions of RPF (top) and mRNA (bottom) reads mapped to each of the three nucleotides in the codons.

(**G**) Pearson's correlation of the RPF (left) and mRNA (right) libraries.

(**H**) The expression of neuronal markers in GFP-positive cells. Each of the neuronal markers are shown on the x-axis. The level of expression is presented as Log2(normalized read counts) on the y-axis. Blue bars represent RPFs of mTOR WT mice; orange bars represent mRNA of WT mice.

(**I**) Pie chart representing functional classification of mTOR activation-sensitive genes in FMCD mice.

Supplemental Figure 4

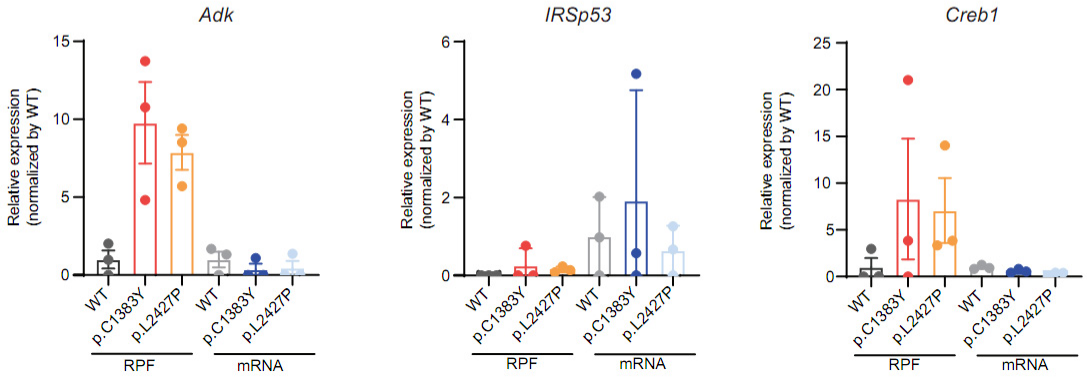

Supplemental Figure 4. Translational activation of *Adk*, *IRSp53*, and *Creb1* in FMCD mice. Bar graphs showing the fold changes in RPF and mRNA of *Adk*, *IRSp53*, and *Creb1* in the WT, p.C1483Y, and p.L2427P mice (n = 3 in each group). Mean ± SD.

Supplemental Figure 5

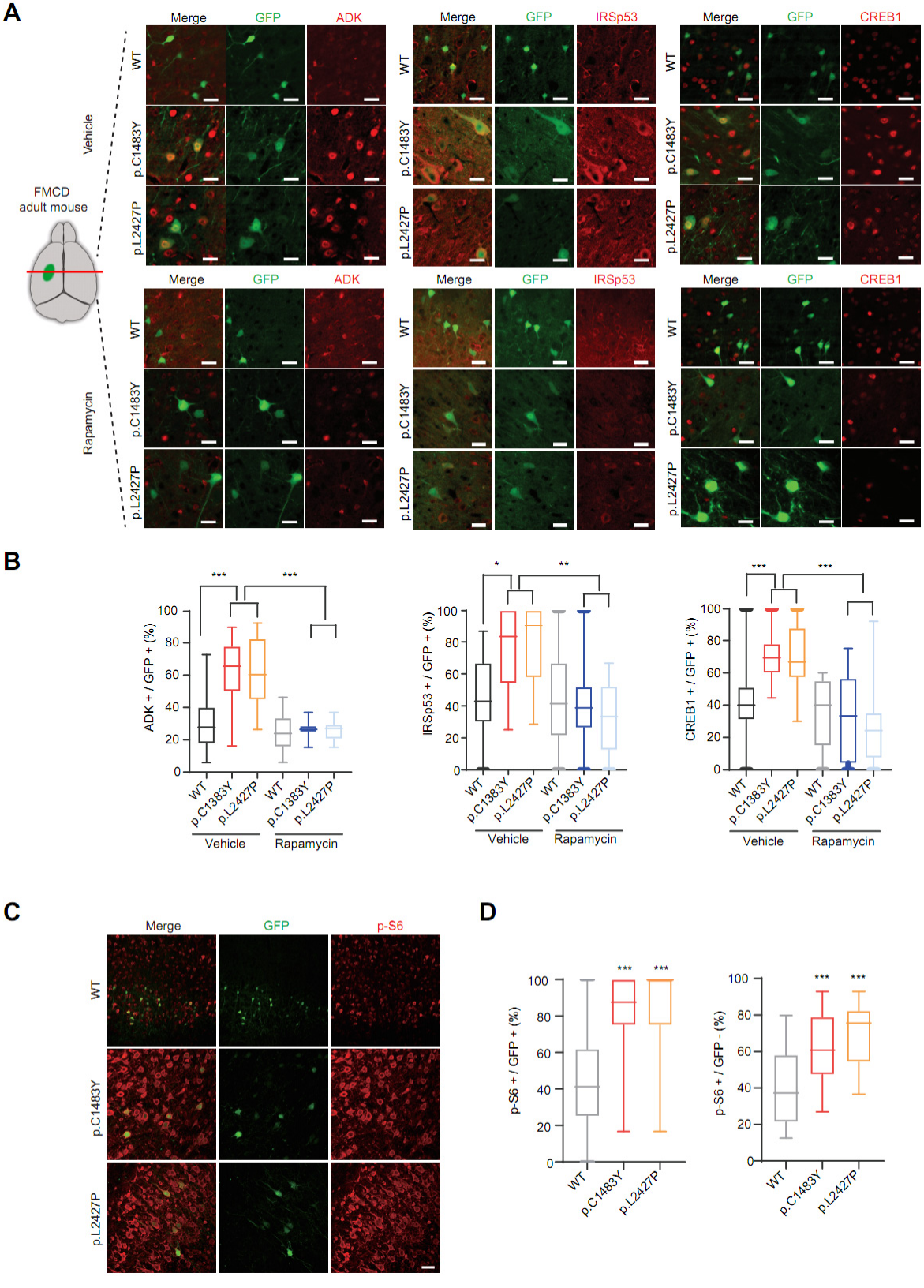

Supplemental Figure 5. The increased expression of ADK, IRSp53, and CREB1 in mTOR activating mutation-carrying neurons is rescued by the treatment of rapamycin in FMCD adult mice.

(**A**) Representative immunofluorescence staining of mTOR activation-sensitive genes (ADK, IRSp53, and CREB1 [red]) in GFP-positive cells (green) from FMCD adult (P56-P140) mice treated with vehicle (top) or rapamycin (bottom). Scale bars, 25 um.

(**B**) Quantification of samples in (**A**). ADK-, IRSp53-, or CREB1 (red)-positivity among GFP-positive cells in the average of two to five representative cortical regions of FMCD mice. * P <0.05, ** P < 0.01, and *** P < 0.001 (n = 5 in each group, one-way analysis of variance [ANOVA] with Bonferroni post-hoc test).

(**C**) Representative immunofluorescence staining of p-S6 (Ser240/244) (red) in FMCD mice (P21). Scale bar, 50 um.

(**D**) Quantification of samples in (**C**). p-S6 (Ser240/244) (red)-positivity among GFP-positive or GFP-negative cells in the average of two to five representative cortical regions of FMCD mice *** P < 0.001 (relative to WT, n = 3 in each group, one-way ANOVA with Bonferroni post-hoc test).

Supplemental Figure 6

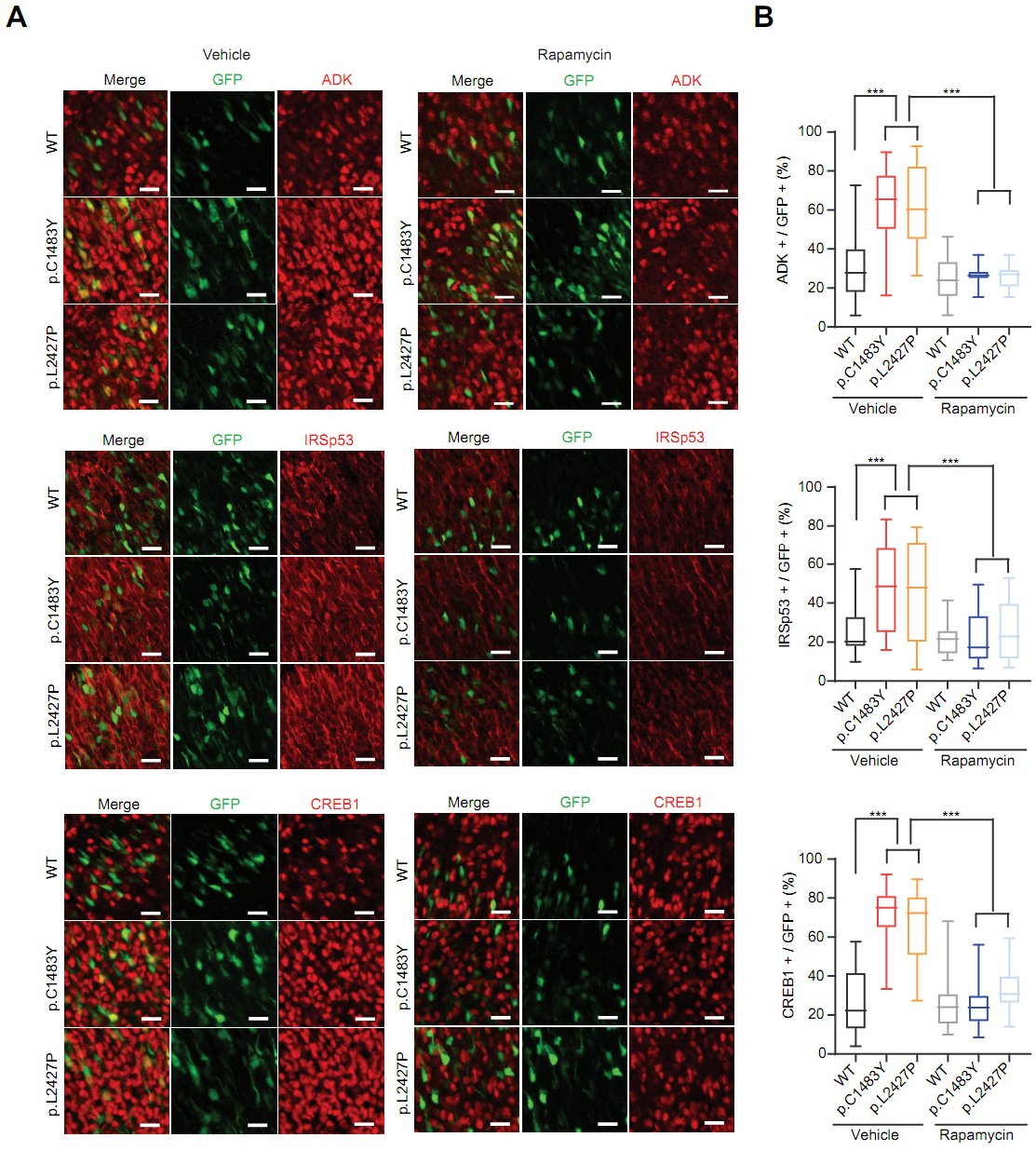

Supplemental Figure 6. The increased expression of ADK, IRSp53, and CREB1 in mTOR activating mutation-carrying neurons is rescued by the treatment of rapamycin in FMCD mice at E18.

(**A**) Representative immunofluorescence staining of mTOR activation-sensitive genes (ADK, IRSp53, and CREB1 [red]) in GFP-positive cells from E18 mice expressing mTOR p.C1483Y

(p.C1483Y) or p.L2427P (p.L2427P) treated with vehicle (left) and rapamycin (right). Scale bars, 25 um.

(**B**) Quantification of (**A**). ADK-, IRSp53-, or CREB1 (red)-positivity among GFP-positive cells in the average of two to five representative cortical regions of FMCD mice. *** $P < 0.001$ (n = 5 in each group, one-way analysis of variance with Bonferroni post-hoc test).

Supplemental Figure 7

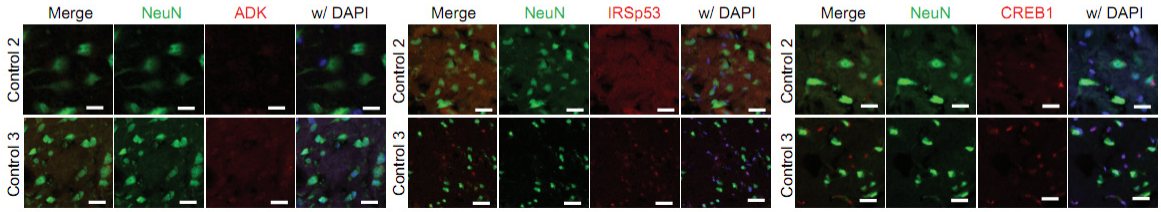

Supplemental Figure 7. The expression of ADK, IRSp53, and CREB1 in brain tissues from control brain tissues. Representative immunofluorescence staining of translationally up-regulated mTOR targets (ADK, IRSp53, and CREB1 [red]) in NeuN+ (green) cells from the patient's brain tissues stained with DAPI (blue). Scale bars, 25 um for ADK and CREB1, 60 um for IRSp53. Control 2 refers to the postmortem brain tissues of UMB5408 and Control 3 refers to the unaffected brain region of FCD247.

Supplemental Figure 8

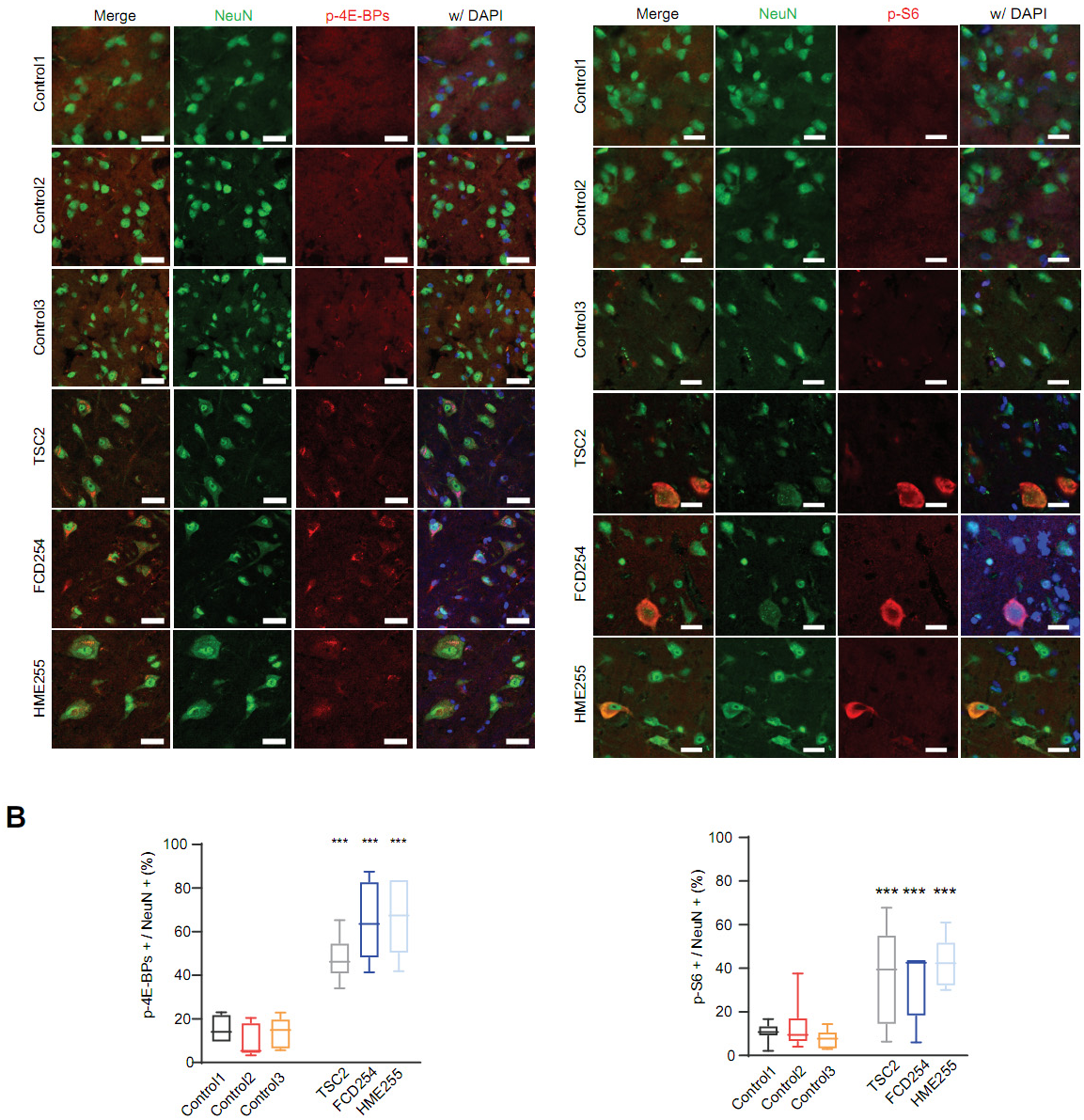

Supplemental Figure 8. The aberrant activation of mTOR kinase in cortical neurons from FMCD patients.

(**A**) Representative immunofluorescence staining of mTOR downstream targets p-4E-BPs (Thr37/46, left) and p-S6 (Ser240/244, right) (red) in NeuN+ (green) cells from FMCD patients. Scale bars, 25 um. Control 1 refers to the postmortem brain tissues of UMB5309, control 2 refers to the postmortem brain tissues of UMB5408, and control 3 refers to the unaffected brain region of FCD247.

(**B**) Quantification of (**A**). Representative cortical regions in each FMCD patient were averaged. * P <0.05, ** P < 0.01, and *** P < 0.001 (one-way analysis of variance with Bonferroni post-hoc test).

Supplemental Figure 9

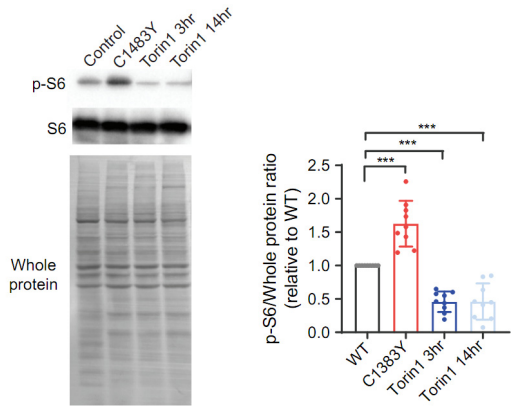

Supplemental Figure 9. The activation and inhibition of mTOR kinase in C1483Y cells and in Torin1 cells. Western blot analysis of p-S6 (Ser240/244), a major read-out of mTOR activation, in C1483Y cells (C1483Y). NIH3T3 cells treated with 200 nM Torin1 for 3 hr (Torin1 3hr) and NIH3T3 cells treated with 200 nM Torin1 for 14 hr (Torin1 14hr). EZblue staining in whole protein lysates were used as loading controls. p-S6 levels are presented as relative ratios to that in control cell lines. *** $P < 0.001$ (n = 9 in each group, one-way analysis of variance with Bonferroni post-hoc test). Mean ± SD.

Supplemental Figure 10

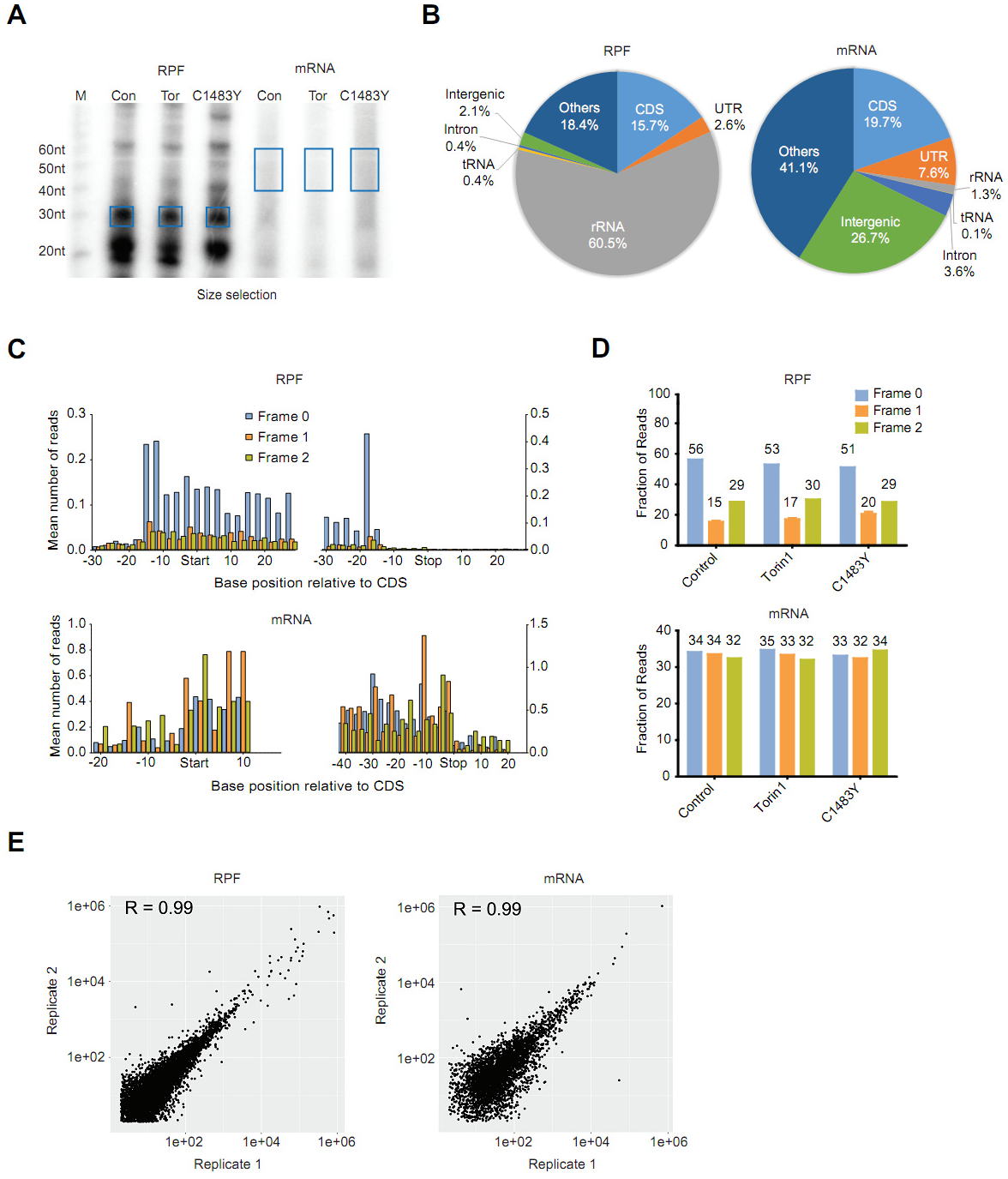

Supplemental Figure 10. Validation of the quality of Ribo-seq and RNA-seq library preparation.

(**A**) Representative images of library preparation of Ribo-seq and RNA-seq upon gel excision during size selection. M: marker, Con: vehicle-treated NIH3T3 WT cells, C1483Y: C1483Y cells, Tor: Torin1 3-hr treated NIH3T3 WT cells.

(**B**) Mapping distributions of read counts for the assigned classes in the RPF (left) and mRNA (right) reads. CDS: coding sequence, UTR: untranslated region.

(**C**) Density of RPF (top) and mRNA (bottom) reads near the translation start and stop codons.

(**D**) Fractions of RPF (top) and mRNA (bottom) reads mapped to each of the three nucleotides in the codons. Three-nucleotide periodicity reflects the movement of ribosomes along mRNA by three nucleotides at a time. Control: control cells, Torin1: Torin1 cells, C1483Y: C1483Y cells.

(**E**) Pearson's correlation of the RPF (left) and mRNA (right) library replicates.

Supplemental Figure 11

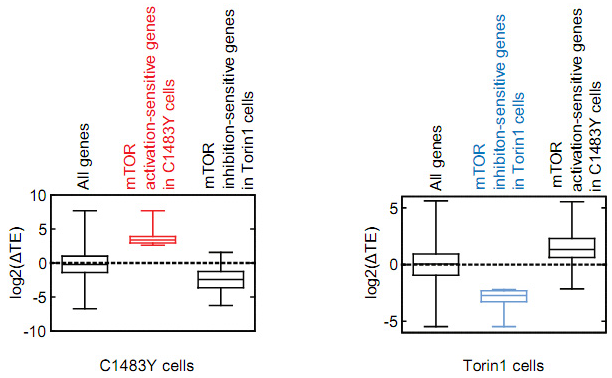

Supplemental Figure 11. Translational profile of mTOR activation-sensitive genes is distinct from that of mTOR inhibition-sensitive genes. Box plots showing the log2 ratios of fold changes (log2[ΔTE]) in the TEs of mRNAs encoding all genes, mTOR inhibition-sensitive genes in Torin1 cells from C1483Y cells (left) and mTOR activation-sensitive genes in C1483Y cells from Torin1 cells (right) relative to control cells.

Supplemental Figure 12

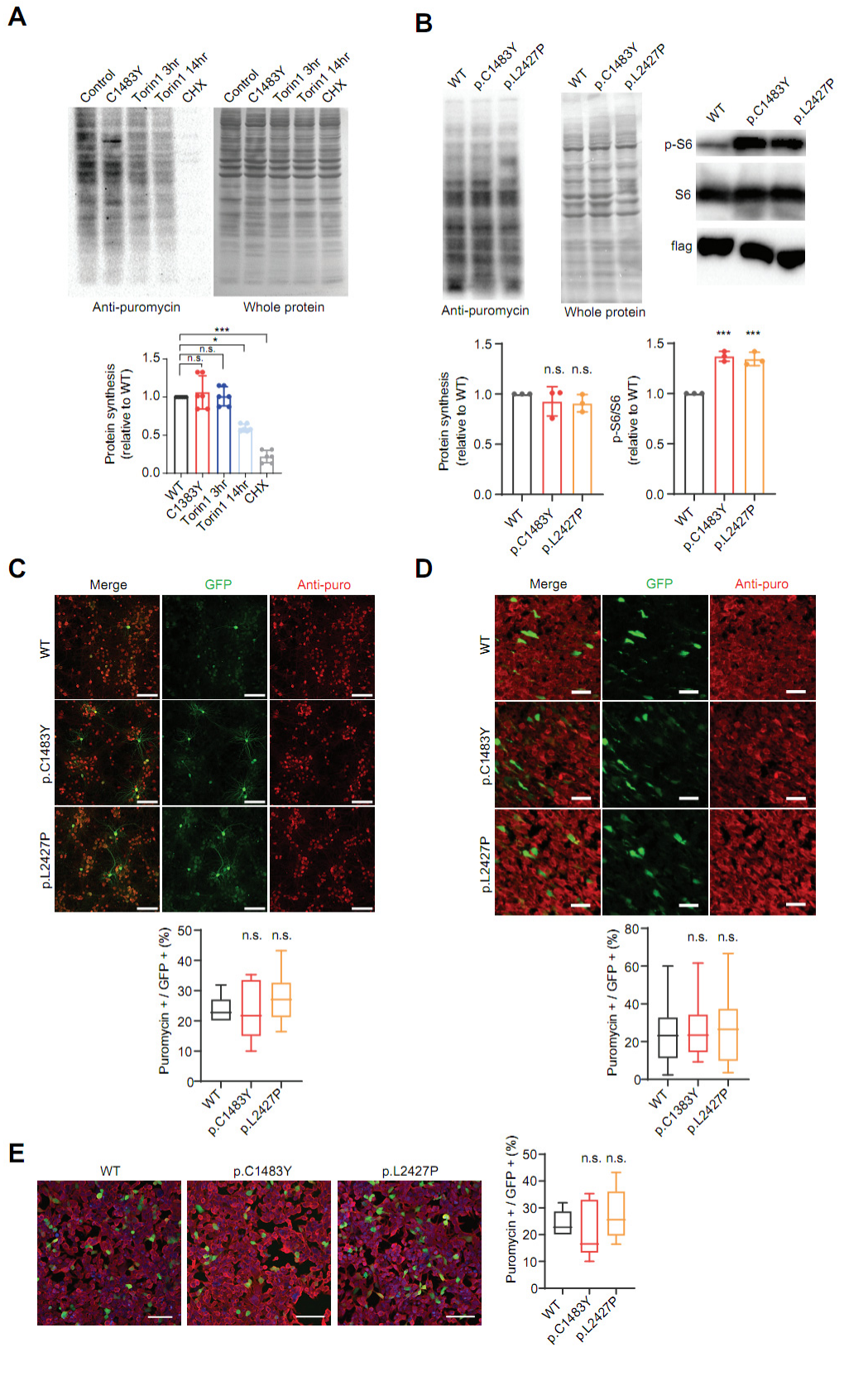

Supplemental Figure 12. Protein synthesis rates are not significantly affected by human *MTOR* mutations *in vitro* and *in vivo*.

(**A**) Western blot and quantification of protein lysates from control cells (Control), C1483Y cells (C1483Y), and Torin1 treated cells (Torin1 3 hr and Torin1 14 hr, 200 nM) to measure basal rates of protein synthesis. EZblue staining in whole protein lysates was used as a loading control. n = 6 in each group. Mean ± SD.

(**B**) Western blot and quantification of protein lysates from flag-mTOR WT (WT), flag-mTOR p.C1483Y (p.C1483Y), or flag-mTOR p.L2427P (p.L2427P) overexpressing HEK293T cells to measure basal rates of protein synthesis. EZblue staining in whole protein lysates was used as a loading control. n = 3 in each group. Mean ± SD.

(**C**) Representative immunofluorescence staining of puromycin incorporated proteins in primary cultured cortical neurons expressing mTOR WT (WT), mTOR p.C1483Y (p.C1483Y), or mTOR p.L2427P (p.L2427P) with GFP-reporter. The level of puromycin incorporation is presented as puromycin positivity in GFP-positive cells. n = 3 in each group. Scale bars, 100 um.

(**D**) Representative immunofluorescence staining of puromycin incorporated proteins in the cortices of E18 mouse embryos expressing mTOR WT (WT), mTOR p.C1483Y (p.C1483Y), or mTOR p.L2427P (p.L2427P) mice with GFP reporter. Puromycin incorporation is presented as puromycin positivity in GFP-positive cells. n = 5 in each group. Scale bars, 30 um.

(**E**) Representative immunofluorescence staining of puromycin incorporated proteins in HEK293T cells expressing mTOR WT (WT), mTOR p.C1483Y (p.C1483Y), or mTOR p.L2427P (p.L2427P) with GFP reporter. The level of puromycin incorporation is presented as puromycin positivity in GFP-positive cells. n = 3 in each group. Scale bars, 200 um.

* $P < 0.05$ and *** $P < 0.001$, one-way ANOVA with Bonferroni post-hoc test

Supplemental Figure 13

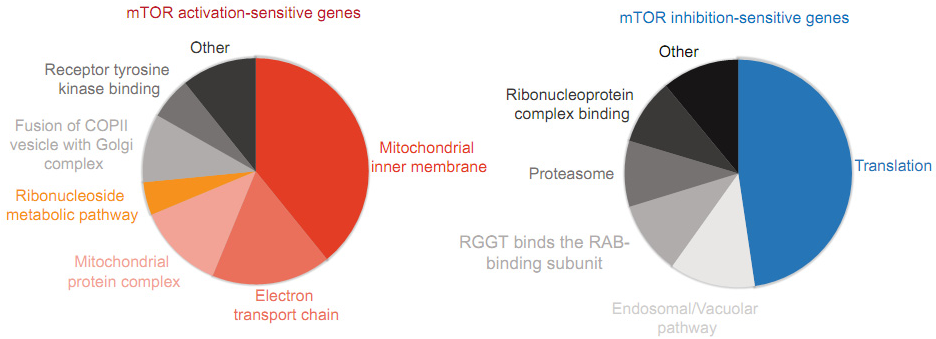

Supplemental Figure 13. Enriched functional clusters of mTOR activation-sensitive genes is distinct from that of mTOR inhibition-sensitive genes. Pie charts represent cluster analysis results of mTOR activation-sensitive genes in C1483Y cells (135 genes with z-score $\geq$ 1.5, top) and mTOR inhibition-sensitive genes in Torin1 cells (144 genes with z-score $\leq$ -1.5, Torin1 down-regulated, bottom). Each functional cluster is significantly enriched in GO terms generated by the ClueGo app in Cytoscape. The size of the pie corresponds to the number of genes.

Supplemental Figure 14

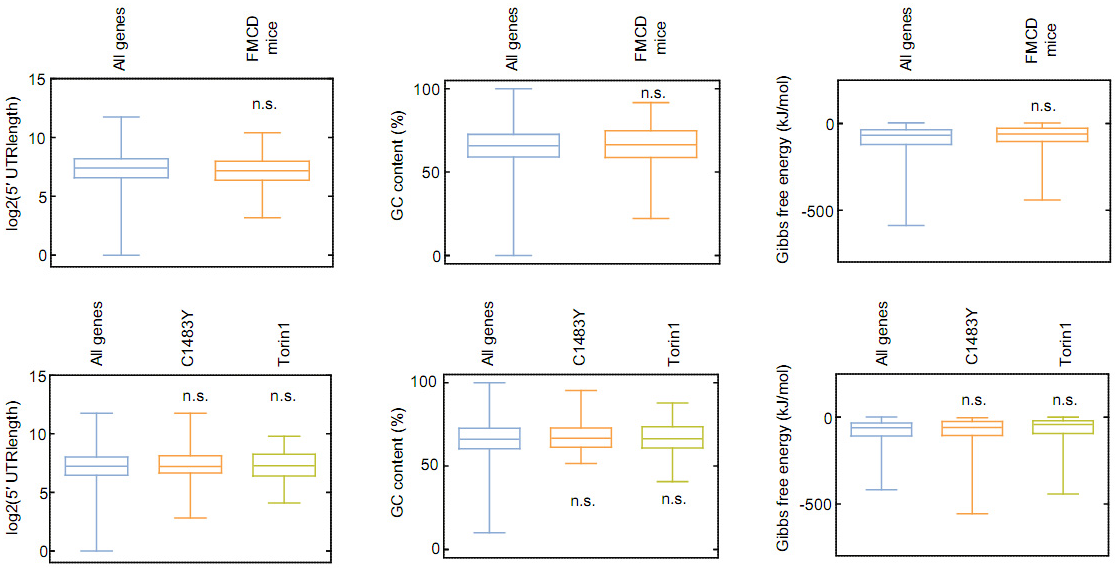

297

298 **Supplemental Figure 14. Canonical 5′ UTR features of mTOR activation- and inhibition-**
299 **sensitive genes.** Comparison of canonical 5′ UTR features between all genes and subsets whose
300 TEs were related with mTOR activation-sensitive genes in the FMCD mice and C1483Y cells
301 (C1483Y) or with mTOR inhibition-sensitive genes in Torin1 cells (Torin1).

302

303

304

305

306

307

308

309

310

Supplemental Figure 15

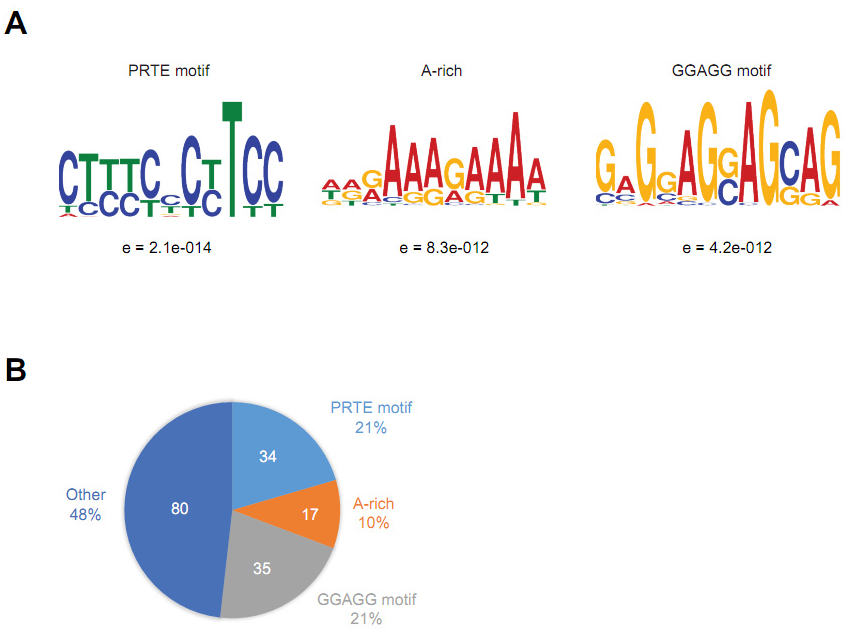

Supplemental Figure 15. 5′ UTR motifs of mTOR inhibition-sensitive genes found in Torin 1 cells.

(**A**) MEME analysis showing consensus sequences and enrichment values (E-value) of the pyrimidine-rich translational element (PRTE), A-rich, and GGAGG motifs of mTOR inhibition-sensitive genes found in Torin1 cells.

(**B**) Diagram illustrating the percentage and number of mTOR inhibition-sensitive genes containing a PRTE, A-rich, or GGAGG motifs.

Supplemental Figure 16

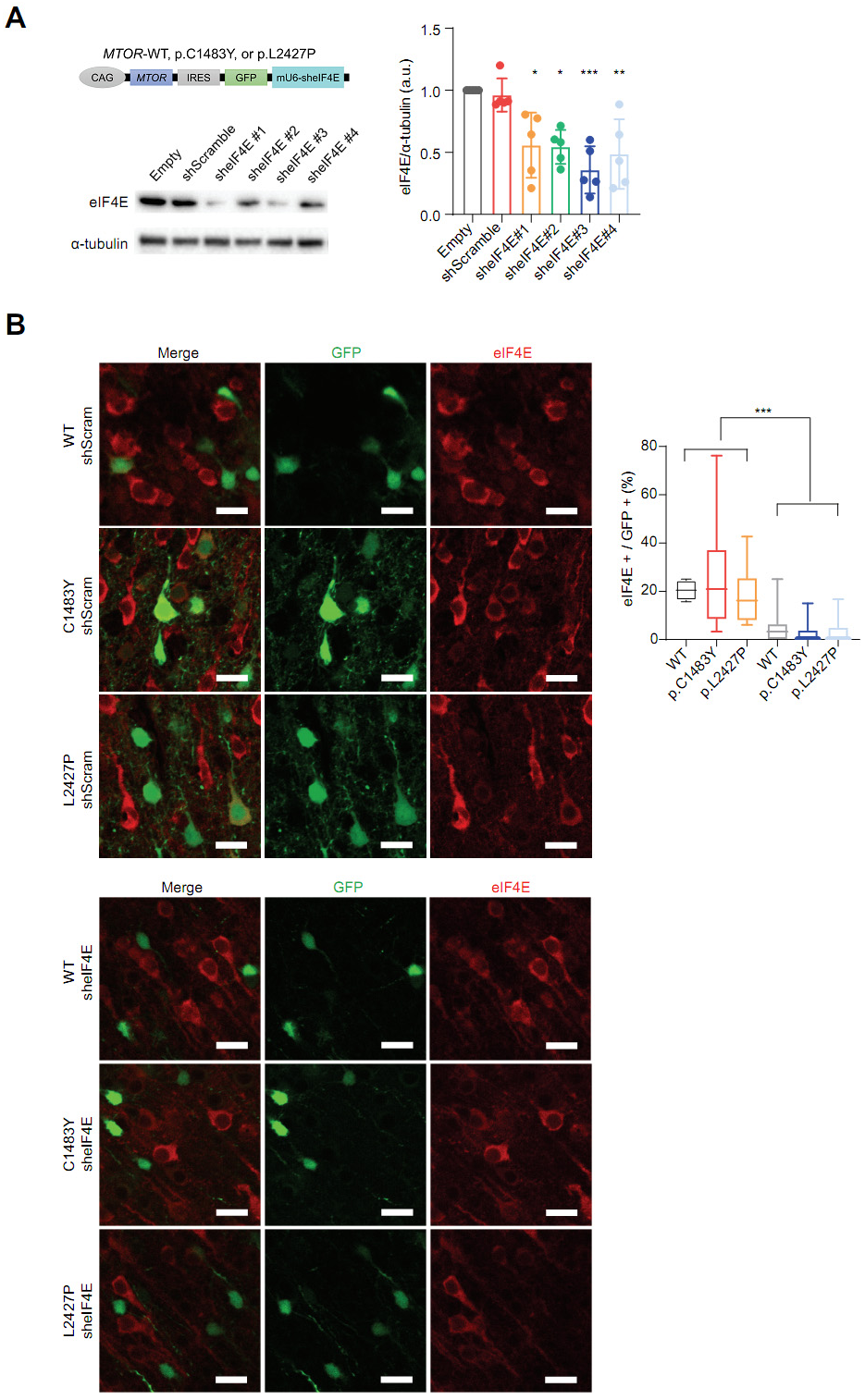

Supplemental Figure 16. The efficient knockdown of eIF4E in FMCD mice.

(**A**) Western blot analysis of eIF4E in sheIF4E RNAs expressing Neuro2A cells. sheIF4E#2 was used for further analysis. Quantification of Western blots relative to empty vector, * $P < 0.05$, ** $P < 0.01$, and *** $P < 0.001$ (n = 5 in each case, one-way ANOVA with Bonferroni post-hoc test). Mean ± SD.

(**B**) Representative images of eIF4E (red) knockdown in GFP-positive cells from P7 FMCD mice electroporated with shScramble (top) or sheIF4E (bottom) RNA expressing vectors. *** $P < 0.001$ (n = 5 in each case, one-way ANOVA with Bonferroni post-hoc test). Scale bar = 20 um. Mean ± SEM.

Supplemental Figure 17

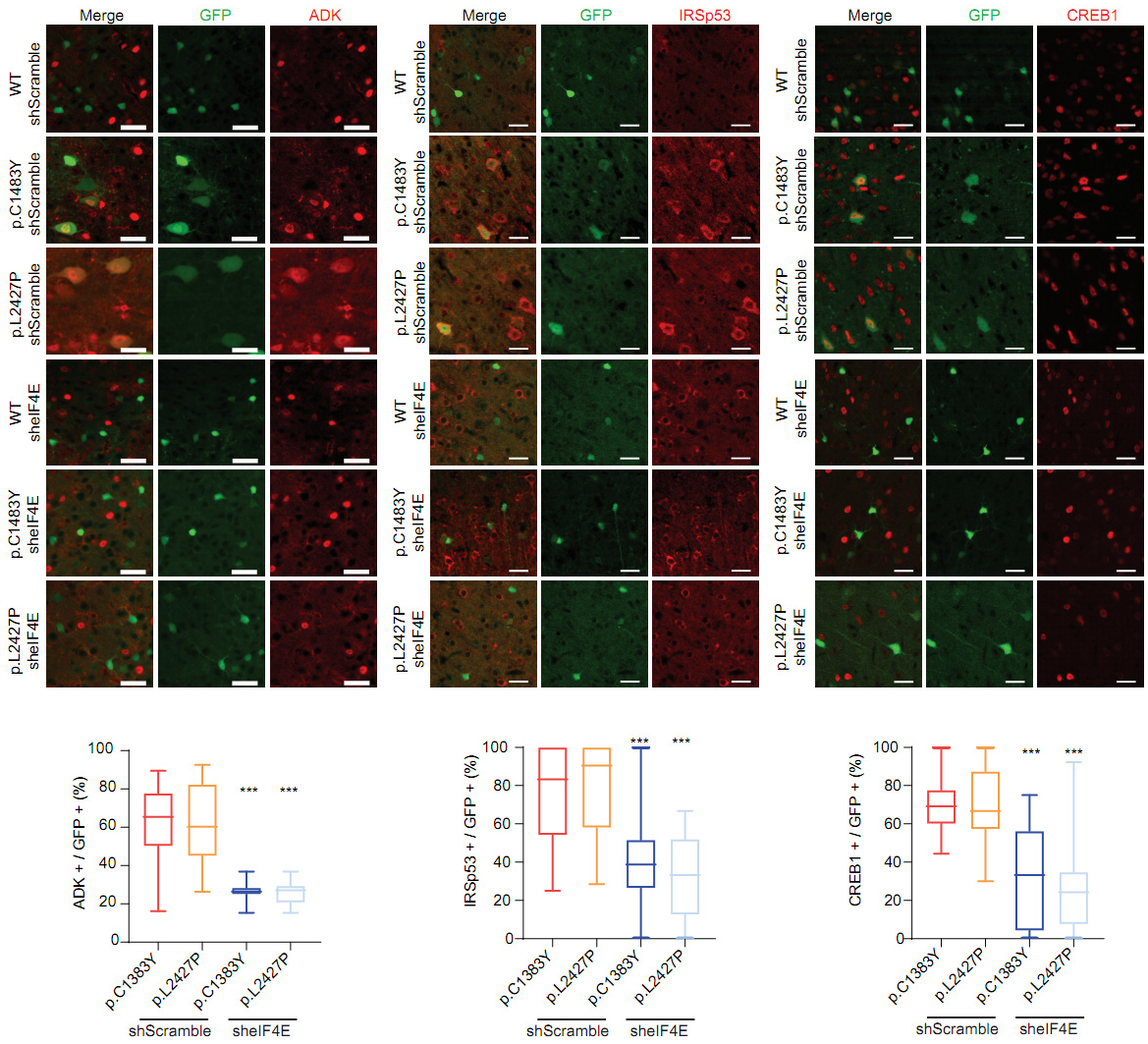

349

350 **Supplemental Figure 17. The increased expression of ADK, IRSp53, and CREB1 in mTOR**
351 **activating mutation-carrying neurons is rescued by the knockdown of eIF4E.** Representative
352 images of ADK, IRSp53, and CREB1 (red) in GFP-positive cells from P21 FMCD mice treated
353 with shScramble (top) or sheIF4E (bottom). *** $P < 0.001$ (n = 5 in each case, one-way analysis
354 of variance [ANOVA] with Bonferroni post-hoc test). Scale bar = 25 um.

355

Supplemental Figure 18

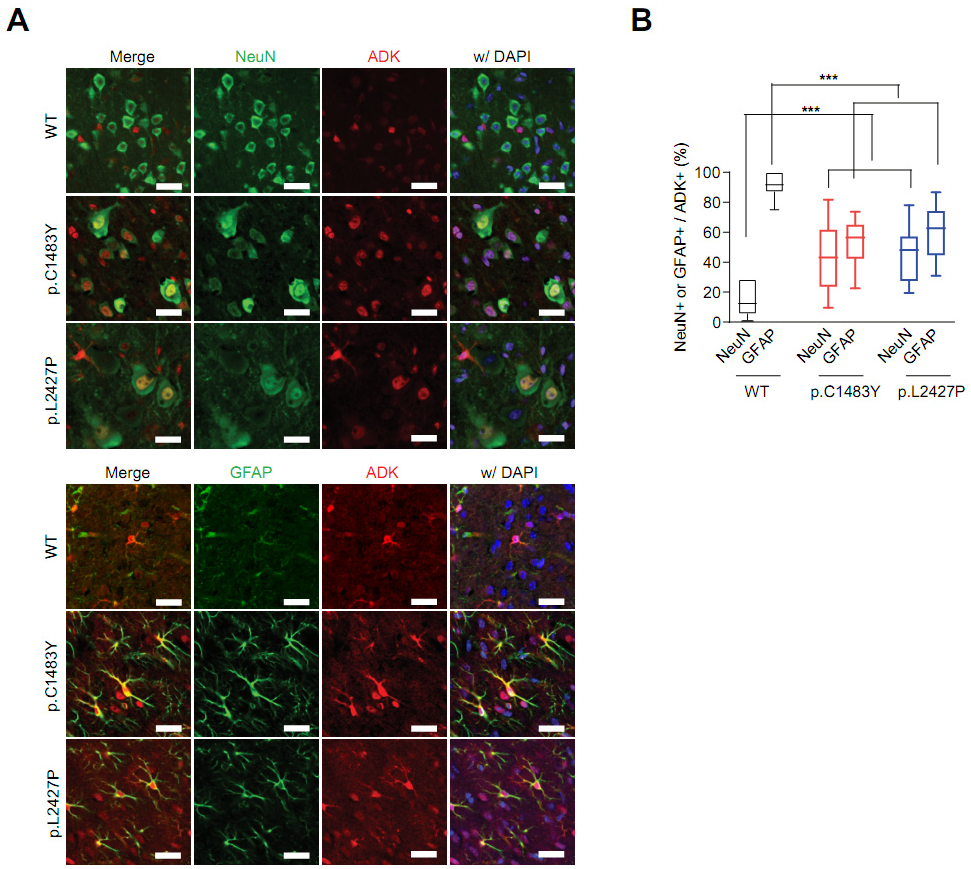

356

357 **Supplemental Figure 18. ADK expression in cortical neurons and astrocytes from FMCD**

358 **mice brains.**

359 (**A**) Representative images of NeuN (green, top) or GFAP (green, bottom) and ADK (red) in GFP-

360 positive cells from adult FMCD model mice (P56-P140).

361 (**B**) Quantification of (A). *** $P < 0.001$ (n = 5 in each case, one-way analysis of variance with

362 Bonferroni post-hoc test). Scale bar = 25 um.

363

364

365

Supplemental Figure 19

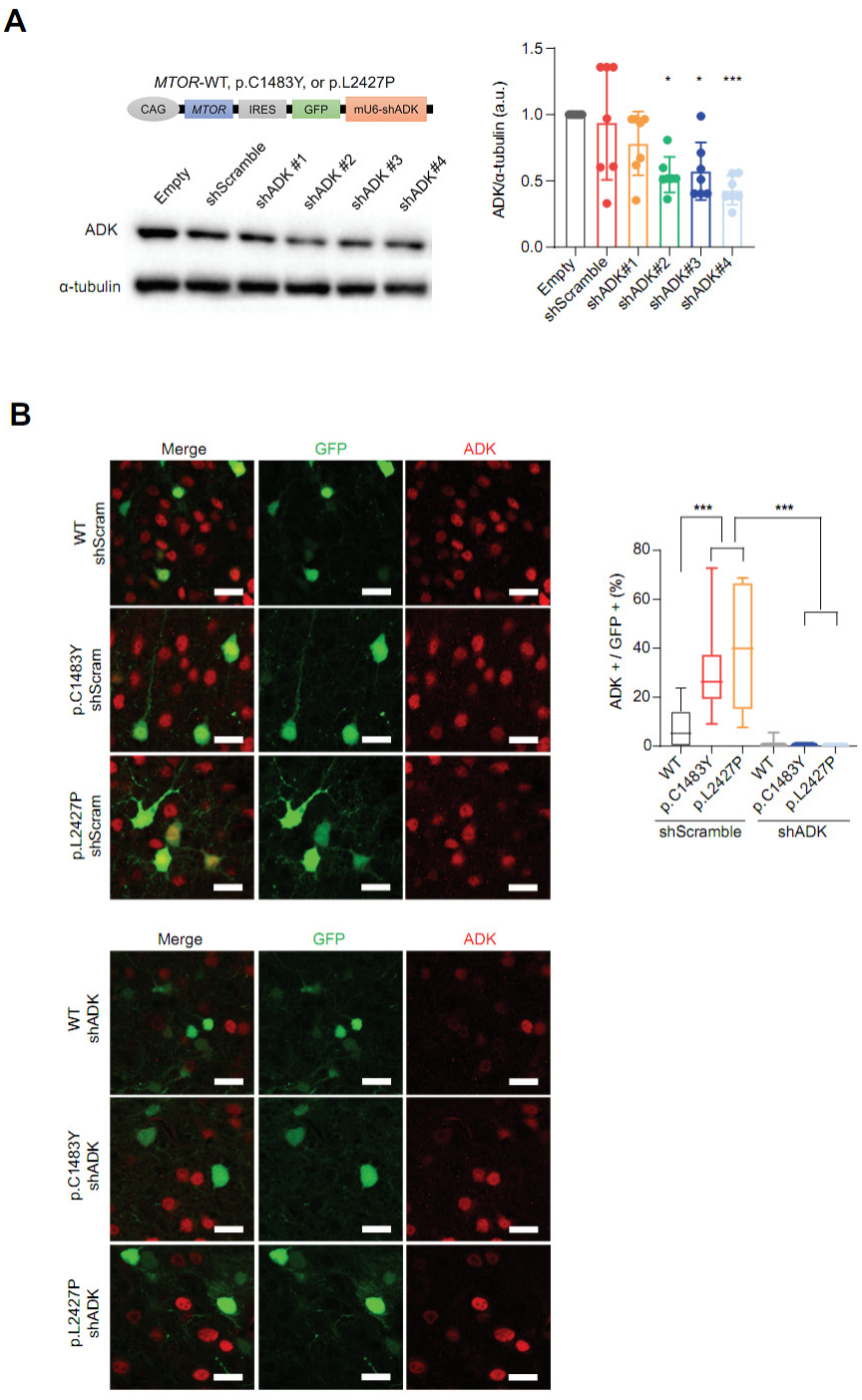

Supplemental Figure 19. The efficient knockdown of ADK in FMCD mice.

(**A**) Western blot analysis to show the efficiency of ADK knockdown in N2A cells. shADK #3 was used for further analysis. Quantification of western blot analysis with the loading control α-tubulin relative to empty vector, * $P < 0.05$ and *** $P < 0.001$ (n = 7 in each case, one-way ANOVA with Bonferroni post-hoc test). Mean ± SD.

(**B**) Representative images of ADK (red) knockdown in GFP-positive cells from P7 FMCD mice electroporated with shScramble (top) or shADK (bottom) RNA expressing vectors. Quantification of ADK knockdown. *** $P < 0.001$ (n = 5 in each case, one-way ANOVA with Bonferroni post-hoc test). Scale bar = 20 um.

Supplemental Table 1.

Mapping distributions of read counts for the assigned classes in the Ribo-seq and RNA-seq libraries of mTOR WT, mTOR p.C1483Y, and mTOR p.L2427P mice.

Class	RPF WT 1st replicate	RPF WT 2nd replicate	RPF WT 3rd replicate	RPF p.C1483Y 1st replicate	RPF p.C1483Y 2nd replicate	RPF p.C1483Y 3rd replicate	RPF p.L2427P 1st replicate	RPF p.L2427P 2nd replicate	RPF p.L2427P 3rd replicate	RNA-seq WT 1st replicate	RNA-seq WT 2nd replicate	RNA-seq WT 3rd replicate	RNA-seq p.C1483Y 1st replicate	RNA-seq p.C1483Y 2nd replicate	RNA-seq p.C1483Y 3rd replicate	RNA-seq p.L2427P 1st replicate	RNA-seq p.L2427P 2nd replicate	RNA-seq p.L2427P 3rd replicate
CDS	8.27%	11.18%	25.40%	9.08%	9.24%	19.40%	15.69%	12.02%	26.71%	29.21%	23.20%	20.03%	30.04%	24.40%	20.99%	26.98%	14.83%	13.02%
UTR	1.96%	1.62%	2.43%	1.28%	1.71%	1.88%	1.88%	1.85%	2.07%	15.77%	12.69%	10.75%	16.58%	13.19%	9.66%	16.37%	8.07%	9.65%
rRNA	50.66%	52.45%	20.20%	18.70%	72.85%	26.33%	46.81%	53.88%	23.22%	1.60%	1.06%	2.31%	1.53%	1.06%	0.99%	1.27%	1.09%	2.10%
tRNA	0.54%	0.36%	0.40%	0.34%	0.20%	0.27%	0.41%	0.32%	0.29%	0.08%	0.03%	0.08%	0.12%	0.04%	0.06%	0.12%	0.03%	0.16%
Intron	0.51%	0.39%	0.85%	1.69%	0.45%	0.55%	0.49%	0.47%	0.85%	5.85%	5.91%	10.69%	5.38%	4.99%	3.69%	6.45%	3.75%	6.91%
Intergenic	2.62%	2.05%	4.70%	2.72%	1.48%	4.18%	2.53%	2.87%	6.10%	29.32%	32.21%	33.42%	24.22%	28.09%	39.32%	32.36%	24.74%	35.97%
Others	35.46%	31.95%	46.01%	66.18%	14.07%	47.39%	32.19%	28.58%	40.76%	18.17%	24.91%	22.73%	22.12%	28.23%	25.31%	16.45%	47.48%	32.19%
Total Reads	78938989	103041083	130980756	243382145	105409798	113437980	81881324	81623538	88549718	101252271	141375625	69976707	114068454	143206719	92636343	131307738	86508443	96911633

adaptor-only were removed from total count

Read count

Class	RPF WT 1st replicate	RPF WT 2nd replicate	RPF WT 3rd replicate	RPF p.C1483Y 1st replicate	RPF p.C1483Y 2nd replicate	RPF p.C1483Y 3rd replicate	RPF p.L2427P 1st replicate	RPF p.L2427P 2nd replicate	RPF p.L2427P 3rd replicate	RNA-seq WT 1st replicate	RNA-seq WT 2nd replicate	RNA-seq WT 3rd replicate	RNA-seq p.C1483Y 1st replicate	RNA-seq p.C1483Y 2nd replicate	RNA-seq p.C1483Y 3rd replicate	RNA-seq p.L2427P 1st replicate	RNA-seq p.L2427P 2nd replicate	RNA-seq p.L2427P 3rd replicate
CDS	6,529,989	11,519,568	33,273,024	22,107,689	9,736,770	22,003,872	12,847,657	9,813,545	23,650,209	29,579,025	32,798,533	14,013,504	34,268,460	34,942,515	19,441,832	35,420,601	12,831,722	12,620,076
UTR	1,544,862	1,673,236	3,181,416	3,119,152	1,802,929	2,128,340	1,541,299	1,507,894	1,836,959	15,962,467	17,939,142	7,524,199	18,911,114	18,893,715	8,944,379	21,490,401	6,980,943	9,350,767
rRNA	39,987,803	54,043,696	26,462,136	45,503,549	76,793,431	29,870,732	38,330,375	43,980,102	20,557,114	1,619,398	1,498,243	1,614,323	1,743,708	1,515,700	913,756	1,671,070	940,309	2,038,728
tRNA	422.791	369.034	529.776	839.309	210.890	307.788	334.210	263.375	255.662	77.451	38.152	54.717	141.801	62.059	57.181	151.954	29.560	151.485
Intron	398,705	399,477	1,112,931	4117726	473,852	627,556	401,804	387,468	754,228	5,927,207	8,353,759	7,478,420	6,142,088	7,144,008	3,416,603	8,472,938	3,243,547	6,696,664
Intergenic	2,065,518	2,115,265	6,159,993	6,616,628	1,562,808	4,736,640	2,070,063	2,345,988	5,402,391	29,684,320	45,533,052	23,385,552	27,626,240	40,226,286	36,420,438	42,495,602	21,405,092	34,858,117
Others	27,989,321	32,920,807	60,261,480	161,078,092	14,829,118	53,763,052	26,355,916	23,325,166	36,093,155	18,402,403	35,214,744	15,905,992	25,235,043	40,422,436	23,442,154	21,605,172	41,077,270	31,195,796
Total Reads	78,938,989	103,041,083	130,980,756	243,382,145	105,409,798	113,437,980	81,881,324	81,623,538	88,549,718	101,252,271	141,375,625	69,976,707	114,068,454	143,206,719	92,636,343	131,307,738	86,508,443	96,911,633

adaptor-only were removed from total count

Supplemental Table 4.

Clinical information of FMCD patients and control cases.

Patient ID	Age	Sex	Age at first seizure	Age at surgery	Seizure frequency	Tissue region	Etc
UMB1712	20Y	male	-	-	-	Frontal	Postmortem tissues
UMB4917	22Y	male	-	-	-	Frontal	Postmortem tissues
UMB5309	14Y	female	-	-	-	Temporal	Postmortem tissues
UMB5408	6Y	male	-	-	-	Temporal	Postmortem tissues
FCD56	10Y	female	2Y	6Y	3/day	Frontal	-
FCD247	11Y	female	1Y	9Y	N.A.	Temporal	-
FCD254	12Y	male	4Y	9Y	10/day	Frontal	-
FCD348	6Y	male	4Y	5Y	N.A.	Frontal	-
HME20	5Y	female	2M	9M	10/day	Frontal	-
HME255	20Y	female	8Y	17Y	3/day	Temporal	-
HME338	17Y	female	5Y	15Y	N.A.	Temporal	-
TSC2	8Y	female	2Y	4Y	N.A.	Temporal	-
TSC264	2Y	female	1Y	1Y	6/day	Frontal	-
TSC357	20Y	male	1Y	18Y	N.A.	Frontal	-

Supplemental Table 5.

mTOR pathway mutations found in FMCD patients

Patient ID	Sequencing	Mutation type	Mutated gene	Nucleotide changes	Protein change	Reference	Altered read	Frequency (%)
TSC2	Whole exome sequencing	Germline	*TSC2*	c.3355C>T	p.Gln1119*	74	43	36.75
FCD254	Targeted hybrid capture sequencing	Somatic	*MTOR*	c.4376C>A	p.Ala1459Asp	882	30	3.29
HME255	Targeted hybrid capture sequencing	Somatic	*MTOR*	c.4448G>A	p.Cys1483Tyr	836	87	9.43
TSC264	Targeted hybrid capture sequencing	Germline	*TSC2*	c.3007delG	p.Ala1003fs	2282	278	10.86
TSC357	Targeted hybrid capture sequencing	Germline	*TSC2*	c.5153A>C	p.His1718Pro	2792	1313	31.99

Supplemental Table 7.

Mapping distributions of read counts for the assigned classes in the Ribo-seq and RNA-seq libraries of C1483Y cells, Torin1 cells, and control cells.

Percent

Class	RPF control 1st replicate	RPF control 2nd replicate	RPF control 3rd replicate	RPF Torin1 1st replicate	RPF Torin1 2nd replicate	RPF Torin1 3rd replicate	RPF C1483Y 1st replicate	RPF C1483Y 2nd replicate	RPF C1483Y 3rd replicate	RNA-seq control 1st replicate	RNA-seq control 2nd replicate	RNA-seq control 3rd replicate	RNA-seq Torin1 1st replicate	RNA-seq Torin1 2nd replicate	RNA-seq Torin1 3rd replicate	RNA-seq C1483Y 1st replicate	RNA-seq C1483Y 2nd replicate	RNA-seq C1483Y 3rd replicate
CDS	14.72%	34.79%	15.48%	17.83%	18.56%	22.90%	6.38%	6.31%	3.86%	27.08%	21.50%	32.30%	13.55%	37.03%	32.82%	3.31%	4.48%	5.41%
UTR	2.26%	1.90%	1.08%	7.42%	1.56%	4.99%	1.43%	0.55%	2.60%	10.35%	9.66%	13.96%	5.41%	13.93%	12.90%	0.63%	0.58%	0.73%
rRNA	79.96%	48.59%	37.65%	69.11%	64.53%	55.54%	59.45%	63.97%	65.57%	1.65%	1.19%	1.39%	2.86%	0.75%	1.04%	1.51%	0.95%	0.64%
tRNA	0.17%	0.48%	0.35%	0.24%	0.19%	0.60%	0.90%	0.27%	0.36%	0.04%	0.05%	0.02%	0.05%	0.01%	0.07%	0.11%	0.09%	0.10%
Intron	0.16%	0.57%	0.27%	0.28%	0.66%	0.81%	0.26%	0.30%	0.15%	4.26%	4.93%	4.89%	2.99%	5.26%	3.48%	1.65%	2.07%	2.53%
Intergenic	0.87%	2.82%	1.39%	1.51%	2.99%	2.38%	2.26%	3.11%	1.27%	27.65%	24.63%	34.29%	20.72%	19.16%	24.90%	44.58%	21.84%	22.30%
Others	1.85%	10.84%	43.77%	3.61%	11.52%	12.77%	29.32%	25.50%	26.19%	28.96%	38.05%	13.15%	54.42%	23.87%	24.80%	48.19%	69.98%	68.30%
Total Reads	84544590	126593842	86026712	69845284	105027922	117489790	67839196	76803583	115448783	76325689	322820203	131345936	68919162	109353253	89619698	132948004	99084567	106717153

Too-short, non-cliped, and adaptor-only were removed from total count

Read count

Class	RPF control 1st replicate	RPF control 2nd replicate	RPF control 3rd replicate	RPF Torin1 1st replicate	RPF Torin1 2nd replicate	RPF Torin1 3rd replicate	RPF C1483Y 1st replicate	RPF C1483Y 2nd replicate	RPF C1483Y 3rd replicate	RNA-seq control 1st replicate	RNA-seq control 2nd replicate	RNA-seq control 3rd replicate	RNA-seq Torin1 1st replicate	RNA-seq Torin1 2nd replicate	RNA-seq Torin1 3rd replicate	RNA-seq C1483Y 1st replicate	RNA-seq C1483Y 2nd replicate	RNA-seq C1483Y 3rd replicate
CDS	12,444,778	44,047,852	13,316,688	12,455,249	19,489,475	26,909,780	4,330,316	4,848,522	4,457,937	20,669,878	69,391,964	42,430,223	9,336,081	40,489,913	29,410,775	4,403,984	4,439,827	5,768,864
UTR	1,906,633	2,408,183	931,792	5,182,850	1,636,157	5,865,303	970,988	420,378	3,004,013	7,897,164	31,197,801	18,330,940	3,728,412	15,231,951	11,556,820	836,686	574,542	777,675
rRNA	67,605,641	61,515,585	32,385,272	48,271,061	67,773,905	65,252,417	40,330,493	49,129,378	75,701,188	1,261,073	3,838,643	1,820,533	1,968,453	819,758	927,610	2,013,234	941,504	680,658
tRNA	145,049	606,121	303,432	168,462	194,961	709,128	611,800	203,921	410,989	34,232	154,145	30,211	35,490	10,598	66,703	152,425	93,897	108,332
Intron	139,050	723,993	232,866	194296	691,553	947,217	173,956	230,197	172,557	3,252,823	15,913,740	6,428,789	2,059,995	5,754,400	3,116,139	2,194,830	2,053,996	2,696,231
Intergenic	739,701	3,574,020	1,200,004	1,051,027	3,138,045	2,796,909	1,530,929	2,387,095	1,471,661	21,107,042	79,496,104	45,030,243	14,203,437	20,940,461	22,313,403	59,273,559	21,609,399	23,796,910
Others	1,563,738	13,718,088	37,656,598	2,521,739	12,103,026	15,007,036	19,890,714	19,584,092	30,230,418	22,102,877	122,827,726	17,266,997	37,507,294	26,098,172	22,228,248	64,073,286	69,341,402	72,888,483
Total Reads	84,544,590	126,593,842	86,026,712	69,845,284	105,027,922	117,489,790	67,839,196	76,803,583	115,448,783	76,325,689	322,820,203	131,345,936	68,919,162	109,353,253	89,619,698	132,948,004	99,084,567	106,717,153

Too-short, non-cliped, and adaptor-only were removed from total count

Supplemental Table 12.

Upstream analysis of mTOR activation-sensitive genes in C1483Y cells.

Upstream Regulator	Molecule Type	Predicted Activation State	Activation z-score	p-value of overlap	Target molecules in dataset
EIF4E	translation regulator	Activated	2.236	0.00271	ATOX1,BIRC6,CDC34,CKS2,NUDT3

Supplemental Table 13.

Summary of 5′ UTR motifs (E-score) identified in subset of mTOR activation-sensitive genes.

5′ UTR motif	*Adk-S*	*Creb1*	*IRSp53*	*Atox1*	*Birc6*	*Cdc34*	*Cks2*	*Nudt3*
$(GGC)_4$	9.07E-05	7.90E-06				5.10E-05		5.51E-06
U-rich			4.61E-05					
A-rich		1.58E-05						
CERT		6.69E-05		1.34E-05	7.42E-05	1.76E-06		2.99E-05

Supplemental Table 2. (Separate file)

Log2 ratio of fold changes in the translational efficiencies (TEs) of mTOR p.C1483Y and mTOR p.L2427P mice relative to mTOR WT mice with z-score.

Supplemental Table 3. (Separate file)

mTOR activation-sensitive genes in FMCD mice.

Supplemental Table 6. (Separate file)

5′ TOP mRNAs and log2 ratio of fold changes in the translational efficiencies (TEs) of mTOR p.C1483Y and mTOR p.L2427P mice relative to mTOR WT mice.

Supplemental Table 8. (Separate file)

Log2 ratios of fold changes in the translational efficiencies (TEs) of C1483Y and Torin1 cells relative to control cells with z-score.

Supplemental Table 9. (Separate file)

5′ TOP mRNAs and log2 ratios of fold changes in the translational efficiencies (TEs) of C1483Y cells and Torin1 cells relative to control cells.

Supplemental Table 10. (Separate file)

Length, GC content, and Gibbs free energy change of 5′ UTRs of mTOR activation- and inhibition-sensitive genes in FMCD mice, C1483Y, and Torin 1 cells.

Supplemental Table 11. (Separate file)

mTOR activation- and inhibition-sensitive genes with identified 5′ UTRs motifs.

Supplemental Table 14. (Separate file)

The sequence of 5′ UTRs and motifs in *Adk-S*, *IRSp53*, and *Creb1* that are deleted in 5′ UTR reporter assay.